Mon. Not. R. astr. Soc. (1992) **256**, *Short Communication*, 53P–58P

The optical polarizations of high- and intermediate-redshift radio galaxies

C. N. Tadhunter,[1] S. M. Scarrott,[2] P. Draper[2] and C. Rolph[2]

[1] *Department of Physics, University of Sheffield, Sheffield S3 7RH*

[2] *Department of Physics, University of Durham, South Road, Durham DH1 3LE*

Accepted 1992 March 21. Received 1992 March 21; in original form 1992 January 21

SUMMARY

Optical polarization measurements are presented for 12 high- and intermediate-redshift radio galaxies ($0.2 < z < 0.85$). The data confirm that large optical polarization is relatively common at high redshifts: five out of seven of the $z > 0.5$ objects with good polarization measurements have their integrated light polarized at the 5–20 per cent level. This result, and the fact that the polarization is frequently oriented perpendicular to the radio axis, suggests that a large fraction of the UV continuum has been scattered out of radiation beams from the AGN by dust or electrons in the high-redshift host galaxies. In contrast, we find that none of the intermediate-redshift ($0.2 < z < 0.5$) objects shows polarization at the > 5 per cent level. It is likely that the implied redshift dependence is largely a consequence of the varying dilution of the polarization by the light from the stars in the haloes of the galaxies – the dilution is least for the high-redshift objects because they are observed in the rest-frame UV – but it is also possible that the scattering ISM is more effective and/or the radiation beams are stronger at high redshifts.

Key words: polarization – galaxies: active – radio continuum: galaxies.

1 INTRODUCTION

One of the most striking features of high-redshift ($z > 0.5$) radio galaxies is that their rest-frame optical/UV colours are significantly bluer than those measured in early-type galaxies at low redshifts (e.g. Lilly & Longair 1984). This result has been interpreted in terms of bursts of star formation (e.g. Lilly & Longair 1984; Chambers & Charlot 1990) and, since the extended UV structures are found to be aligned with extended radio structures (McCarthy *et al.* 1987), it has been suggested that these starbursts are induced by the passage of the radio jets through the interstellar medium (ISM) in the host galaxies (e.g. Rees 1989; de Young 1989).

Starbursts are not, however, the only way of explaining the UV colours and the alignment effect. The unified schemes for radio sources predict that the radio emission is beamed in the direction of collimation of the plasma jets (e.g. Orr & Browne 1984), and studies of the extended emission-line regions around several low-redshift active galactic nuclei (AGN) indicate that the anisotropy in the radiation field is also present at optical/UV/X-ray wavelengths (see Tadhunter 1990 for a review). Among the low-redshift radio galaxies perhaps the best evidence for such anisotropy is found in PKS 2152 – 69, where a high-ionization emission-line cloud is associated with a blue, polarized continuum source (Tadhunter *et al.* 1988a; di Serego Alighieri *et al.* 1988). The most plausible explanation for the properties of the cloud is that it is intercepting an intense beam of radiation from the nucleus: the high ionization state is induced by the EUV/X-ray radiation in the beam, while the blue continuum source represents light that has been scattered out of the beam by dust in the cloud (di Serego Alighieri *et al.* 1988). The relevance to high-redshift objects is that, if we were to observe PKS 2152 – 69 in the UV, it would show similar aligned UV and radio structures. This similarity led Tadhunter *et al.* (1988b) to propose a beaming/scattering model for the high-redshift galaxies. Fabian (1989) has also suggested an electron scattering model, based on observations of massive X-ray emitting haloes of gas around radio galaxies and quasars.

Over the last few years, attempts have been made to test the beaming/scattering model at high redshifts by searching for the large polarizations expected in the case of scattered light. The results have been encouraging in the sense that the three high-redshift radio galaxies for which polarization measurements have been made all show polarization at the 9–20 per cent level in the UV, with *E*-vectors roughly perpendicular to the extended UV structures (di Serego

Alighieri *et al.* 1989; Scarrott, Rolph & Tadhunter 1990; Januzzi & Elston 1991). However, since two of the measured galaxies are rather extreme in their emission-line properties (3C265 and 368), the criticism might be levelled that these objects are not typical of the population of high-redshift 3C radio galaxies and that the high UV polarizations are not a general phenomenon. Furthermore, because few measurements exist of the optical/UV polarizations of intermediate-redshift radio galaxies ($0.2 < z < 0.5$), the redshift dependence of the polarization is not clear.

In this paper we present polarization measurements of 12 powerful radio galaxies covering the intermediate- to high-redshift range ($0.2 < z < 0.85$) and with emission-line luminosities that are typical of the general population of 3C radio galaxies. We discuss the results in the context of models for the formation of the UV continuum in radio galaxies.

2 OBSERVATIONS

The observations were made with the Durham polarimeter in three runs on La Palma: two with the William Herschel Telescope (WHT) (1989 July and 1991 January) and one with the Isaac Newton Telescope (INT) (1991 August). Details are given in Table 1.

The Durham polarimeter is described in Scarrott *et al.* (1983) and uses a CCD detector system based on the GEC P8600 chip (Wright & MacKay 1981). Three bandpasses were used for the observations: a standard (Johnston) V (V in Table 1), a 'broad' V (V' in Table 1) and no filter (NF in Table 1). The V and V' filters have approximate central wavelengths and widths (FWHM) of 5520/860 and 5560/1350 Å, respectively, while the bandpass for the no-filter observations of 3C441 is less certain and is defined by the spectral response of the CCD, which peaks at ~6500 Å and has an effective FWHM of ~2000 Å, and by the spectral energy distribution of the galaxy, which is likely to rise steeply to the red.

The data were reduced using the standard procedures outlined in Scarrott *et al.* (1983) and Draper (1988). Although most of the selected objects were well out of the Galactic plane, we checked for a contribution to the polarization from the local ISM by measuring the polarizations of stars and galaxies in the fields of the objects; no evidence was found for such a contribution in any object.

With the exception of PKS 0116+08 (see Spinrad *et al.* 1976), all the objects were selected from the Spinrad *et al.* (1985) catalogue of 3C radio galaxies. Some basic properties for the galaxies are listed in the last two columns of Table 1. The sample was chosen without reference to the extended nature of the galaxies, or to whether the galaxies show the alignment effect noted by McCarthy *et al.* (1987). Although the sample is not in any way complete, it is representative in the sense that the emission-line luminosities cover the range expected for 3C galaxies at redshifts $0.2 < z < 0.85$ (e.g. McCarthy 1987).

3 RESULTS

3.1 General polarization properties of radio galaxies

The polarization results derived from the new data are shown in Table 2. For comparison we also include the three existing measurements for high-redshift radio galaxies from the literature, and our recent measurement of the highly luminous but radio-quiet *IRAS* galaxy F10214+4724 (see Lawrence *et al.* 1992). The new measurements represent the integrated polarizations for the galaxies in 2-arcsec diameter circular apertures centred on the nuclei. This aperture corresponds to metric diameters $8.9 < D < 20.6$ kpc for $0.2 < z < 0.85$, assuming $H_0 = 50$ km s^{-1} Mpc^{-1} and $q_0 = 0.0$.

A clear feature to emerge from this table is that large (>5 per cent) polarization is relatively common among high-redshift radio galaxies measured in the optical (rest-frame UV); most of the $z > 0.5$ galaxies are highly polarized. The only exceptions are 3C441 and 343.1, but there are mitigat-

Table 1. Details of the imaging polarimetry observations and basic information for the galaxies observed. The times given in column 5 are the total exposure times (for all the half-wave plate positions added together), and details of the filters used are given in the text. The last column gives the log of the [O II](λ3727) emission-line luminosity (erg s^{-1}). For comparison, 3C radio galaxies in the redshift ranges $0.2 < z < 0.3$ and $0.6 < z < 0.9$ have respective mean log[O II] luminosities of 42.0 and 43.2 (data from compilation in McCarthy 1987); 3C368, 265 and 277.2 (see Table 2) have respective mean log[O II] luminosities of 44.06, 44.12 and 43.48.

Object	Date	Tel.	Filt.	t(s)	z	[OII]
3C17	08/91	INT	V'	2400	0.2197	42.10
3C42	08/91	INT	V'	5600	0.395	
PKS0116+08	08/91	INT	V'	4800	0.5936	43.15
3C171	01/91	WHT	V	2400	0.2384	42.68
3C226	01/91	WHT	V	3600	0.823	43.01
3C343.1	08/91	INT	V'	3600	0.750	42.71
3C379.1	08/91	INT	V'	2000	0.256	
3C411	08/91	INT	V'	3600	0.467	
3C441	07/89	WHT	NF	3600	0.707	42.69
3C456	08/91	INT	V'	3600	0.233	
3C459	08/91	INT	V'	3600	0.2199	42.43
3C460	08/91	INT	V'	2000	0.268	41.62
F10214+4724	01/91	WHT	NF	4000	2.28	

Table 2. Polarization measurements for the galaxies in Table 1 and high-redshift galaxies from the literature. Significant measurements ($\delta P/P < 0.5$) are highlighted in bold type. The penultimate column gives the position angle of the radio axis, while the last column gives the position angle difference between the polarization and the radio axes (only calculated for the objects with significant polarization measurements).

Object	z	P(%)	δP	Θ_p°	δΘ°	Θ_{rad}°	$\lvert\Theta_p-\Theta_r\rvert$
3C17	**0.2197**	**2.10**	**0.5**	**60**	**8**	**149**	**89**
3C459	**0.2199**	**1.1**	**0.4**	**33**	**10**	**94**	**61**
3C456	0.233	1.4	0.5	71	11	---	
3C171	0.2384	0.79	0.9	84	32	101	
3C379.1	0.256	1.4	0.8	47	16	108	
3C460	0.268	1.7	1.0	62	17	36	
3C42	**0.395**	**3.5**	**0.5**	**10**	**4**	**124**	**114**
3C411	0.467	1.8	1.3	59	21	112	
P0116+08	**0.5936**	**5.4**	**0.6**	**75**	**3**	**---**	
3C441(NF)	**0.707**	**1.5**	**0.7**	**70**	**13**	**149**	**79**
3C343.1	0.750	1.7	3.0	73	56	98	
3C226	**0.823**	**13.3**	**4.2**	**41**	**9**	**144**	**103**
3C265(B)	**0.811**	**9.2**	**2.1**	**55.9**	**6.5**	**107**	**57**
3C277.2(B)	**0.766**	**21**	**4**	**164**	**6**	**61**	**103**
3C368	**1.132**	**10.1**	**1.8**	**104**	**5**	**18**	**86**
F10214	**2.28**	**16.2**	**1.8**	**75**	**3**	**110**	**35**

References: 3C277.2; di Serego Alighieri *et al.* 1989; 3C265; Januzzi & Elston 1991; 3C368; Scarrott *et al.* 1990; F10214; Lawrence *et al.* 1992.

ing circumstances in both of these cases. First, 3C441 was measured without a filter, which means that the measurement is strongly biased to the red. In fact, we have effectively measured 3C441 in the same rest-wavelength range as the intermediate-redshift radio galaxies. Secondly, we note that the error in the measurement for 3C343.1 is large enough that we cannot rule out $P>5$ per cent in this case. 3C343.1 also differs from the other high-redshift objects (with the possible exception of PKS 0116 + 08), in that it is a compact steep-spectrum radio source, whereas the others are classic double sources. Clearly, both 3C441 and 3C343.1 require further investigation.

There is also evidence for a redshift dependence to the polarization, in the sense that the occurrence of large optical polarization appears to increase with redshift. This is apparent in Fig. 1(a), where we have plotted percentage polarization as a function of redshift. For consistency, this diagram only includes data taken with the Durham polarimeter and reduced using our standard reduction technique.

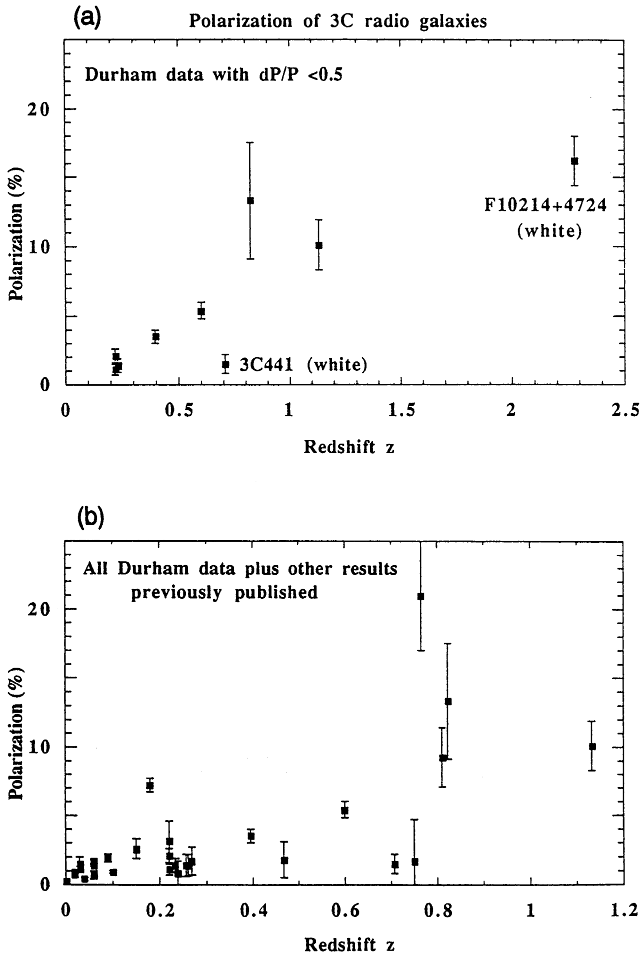

Figure 1. Polarization as a function of redshift for powerful radio galaxies. (a) Durham polarimeter data, $\delta P/P<0.5$; (b) all the Durham polarimeter data plus data from the literature for 3C radio galaxies (no restriction on error). Most measurements are for the V or B wavebands, except for 3C441 and F10214 which were measured without a filter (marked 'white' on diagram). References for 3C radio galaxy data: Antonucci (1984), Tadhunter *et al.* (1990), Draper, Scarrott & Tadhunter (in preparation).

In Fig. 1(b) we have plotted the same diagram, but have included all the polarization data we could find in the literature for 3C radio galaxies. Quasars, blazars and BL Lac objects have been excluded from the diagram, because there are good reasons to believe that they form a distinct group in terms of the optical emission mechanism, but we have retained the low-redshift objects classified as Broad Line Radio Galaxies (BLRG). The diagram therefore includes all objects usually classified as radio galaxies; all are dominated by steep-spectrum radio components, and most have the classic double radio structure.

Some caution is required in interpreting Figs 1(a) and (b), because the data are heterogeneous. Notably, the equivalent metric aperture sizes increase rapidly as a function of redshift – for the highest redshift radio galaxies the apertures include the bulk of the integrated light from the galaxies (tens of kpc), whereas at low redshifts the measurements refer to the immediate vicinities of the nuclei (the inner few kpc). Can the redshift dependence of the polarization apparent in Fig. 1 be a result of this aperture effect? The answer is probably no: although some low-redshift radio galaxies are known to have regions of enhanced polarization off-nucleus (e.g. PKS 2152 – 69), in general, these regions contribute only a small fraction of the integrated light of the galaxy at optical rest-frame wavelengths (~ 1 per cent in the case of the polarized blob in PKS 2152 – 69). Indeed, direct measurements from our imaging polarimetry observations of low- and intermediate-redshift radio galaxies show no evidence for a rise in polarization with aperture size. Quite the reverse is true – the polarization tends to drop because of the diluting effects of the galaxies' haloes, and most of the polarized flux is found near the nuclei of the galaxies, within a radius of a few kpc. The only object in which we have found a large fraction of the light in a polarized component away from the nucleus is the high-z radio galaxy 3C368 (Scarrott *et al.* 1990), but the immediate nuclear region in that object is also highly polarized.

We should also consider the possible dilution of the polarized continuum radiation by emission lines. If such dilution is more important in the low-redshift objects, then it might explain some of the redshift dependence of the polarization. However, there are two reasons for believing that this effect is not a major factor in determining the form of Figs 1(a) and (b). First, many of the measurements for the low-redshift radio galaxies are derived from spectropolarimetry observations which discriminate clearly between emission lines and continuum. Secondly, there is a correlation between emission-line luminosity and radio power/redshift, so the emission-line luminosities in the low-redshift objects are naturally lower than those in the high-redshift objects. From examination of the available spectra, we estimate that the emission-line dilution is unlikely to exceed 30 per cent in any of the $z<0.5$ galaxies.

We will postpone the discussion of other selection effects to Section 4.3. Here we just state that there is a clear increase in the incidence of large optical polarization as the redshift increases, which cannot readily be explained in terms of the effective change in metric aperture size or varying dilution of the polarized continuum by emission lines. The only known example of a $z<0.5$ radio galaxy with $P>5$ per cent is 3C234 ($z=0.185$); and most of the known radio galaxies with $P>5$ per cent lie at $z>0.5$.

3.2 Alignments

Fig. 2 shows the distribution of the difference between polarization and radio axis position angles (PAs) for all $z>0.2$ radio galaxies in which significant polarization has been detected. This shows a clear tendency for the polarization *E*-vectors to be aligned perpendicular to the radio axes. Using a two-sided Kolmogorov–Smirnov test we find that the difference between Fig. 2 and the uniform distribution expected in the case of random orientation of the axes is significant at the >99 per cent level.

It is interesting to compare this result with that of Antonucci (1984) for low-redshift radio galaxies. He found that the radio galaxies fall into two broad groups: one with the polarization perpendicular to the radio axis, the other with the polarization parallel to the radio axis, with a roughly equal division between the two groups. The parallel group tends to be associated with relatively low levels of polarization – at a level of a few per cent or less (Antonucci 1984). This may help to explain why no parallel group members have so far been identified at intermediate/high redshifts: at such redshifts it is difficult to measure the orientation of the polarization accurately enough if the level of polarization is low. Thus, at least some of the objects for which we have failed to measure significant polarization may have low, parallel polarizations. It may be possible to distinguish such objects from the fact that they tend to have relatively strong radio cores (see table 5 of Antonucci 1984). Based on this criterion, 3C411 ($z=0.467$) is a prime candidate for an object with a low, parallel polarization among the galaxies in Table 2.

4 DISCUSSION

4.1 The nature of the UV continuum in high-z radio galaxies

Our observation that many high-redshift radio galaxies are strongly polarized in the (rest frame) UV has important implications for our understanding of the continuum emission mechanism in these objects. Although it has been generally assumed that the UV continuum at high redshifts originates solely in young stars, our observation of significant polarization indicates that we are not seeing direct starlight at these wavelengths. To be highly polarized the starlight would have to be involved in some other secondary process *en route* which induces polarization. One possibility is dichroic extinction by aligned grains in the host galaxy; however, if this mechanism has the same characteristics as observed in the Galaxy it will be most inefficient at the UV rest wavelengths observed in the high-z galaxies, and would require unacceptable levels of extinction. We discard the possibility of a significant contribution from this process in the present situation.

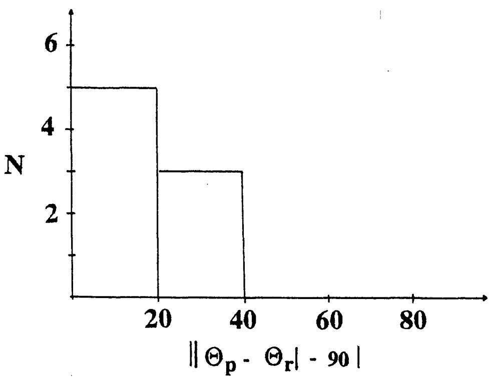

Figure 2. The distribution of position angle differences for powerful radio galaxies with $z>0.2$ and $\delta P/P<0.5$ (includes data from the literature).

An alternative process is the scattering of light by dust grains, and this could be quite significant in the UV, as we know that the scattering cross-sections increase rapidly at shorter wavelengths (*cf.* the terrestrial blue sky). The observed circular patterns and levels of polarization in 3C368 and Cygnus A provide direct evidence for scattering and for the reflection nebula hypothesis, whereby light from a central source is scattered by the surrounding and extended dust distributions in the host galaxy (Scarrott *et al.* 1990; Tadhunter, Scarrott & Rolph 1990). If this hypothesis is generally valid for high-z galaxies then the illuminating source cannot extend throughout the galaxy (as a population of young stars might for instance), but must be highly localized as a hidden AGN.

Our interpretation of the current polarization measurements implies that at least some of the light reaching us has been scattered, but how much? This depends on the dust grains, scattering geometry etc. In the totally extreme and ideal situation of optically thin scattering by Rayleigh grains (or electrons) at a unique angle of 90° the polarization would be 100 per cent, which would mean that any observed percentage polarization would represent the amount of scattered light, i.e. 10 per cent polarization would indicate that 10 per cent of the light has been scattered and 90 per cent is direct. In the more realistic scattering scenario, as typified by Galactic reflection nebulae containing the usual mix of ISM grains, the maximum *spatially resolved* polarizations are usually 30–40 per cent even though all the light is scattered (e.g. Warren-Smith *et al.* 1980; Mannion & Scarrott 1984). Furthermore, the polarizations of the *integrated light* from the nebulae are generally much less than this, because there is some cancelling of the polarizations from different parts of the nebulae. Therefore, if the high-z galaxies have similar dust scattering properties to the Galactic reflection nebulae, then one might conjecture that *the percentage of scattered light is at least a factor of 2–3 times higher than the observed percentage of polarization.*

The evidence in favour of a significant stellar contribution in the rest-frame UV includes the observation of stellar absorption features in the UV continua of some high-z radio galaxies, and a downturn in the continuum at $\lambda<2000$ Å (McCarthy & Chambers 1990).* At longer wavelengths (rest-frame optical/near-IR), the observed dilution of the off-nuclear polarization in 3C368 (Scarrott *et al.* 1990), and the extended infrared structures that are aligned with the radio axes in some cases (Chambers *et al.* 1988; Eisenhart & Chokshi 1990, but see also Rigler *et al.* 1992), also suggest a significant stellar contribution.

*Note that both of these features can also be reconciled with the scattering picture: the absorption feature at 1840 Å can be formed by ISM absorption as well as in stellar atmospheres, while the downturn in continuum is predicted by some dust scattering models.

To resolve this key issue of the proportion of scattered light, we require accurate measurements of the *detailed* stellar continuum features and spectral energy distributions. The existing data on the spectral energy distributions are rather crude, especially in the wavelength range 3000–5500 Å which represents the transition between the UV (dominated by scattered light and/or young stars) and the IR (dominated by old stars?).

4.2 Relevance to the unified schemes

In our earlier work on 3C368, we showed that the extended nebulosity was likely to be illuminated by a hidden AGN of quasar-like luminosity (see Tadhunter 1990). This fits in with many of the unified schemes for AGN, which predict that the radiation for the AGN is emitted anisotropically, such that the appearance of the active galaxy depends on the orientation, and all powerful radio galaxies would have the appearance of quasars if viewed from the direction of the radio axis (e.g. Barthel 1989).

3C368 is the only high-redshift radio galaxy in which we resolve the reflection nebulosity, but the large integrated polarizations in many of the other high-redshift objects are also consistent with the unified schemes. For scattered light, such large percentage polarizations can arise only in the case of anisotropic scattering geometries; in the near-isotropic case (circularly symmetric geometry), the degree of polarization in the integrated light is small because the E-vectors from the different parts of the nebulosity cancel. Thus, the large polarizations are evidence for anisotropies in the reflection nebulae, and the alignment of the E-vectors roughly perpendicular to the radio axes (Fig. 2) shows that the anisotropies are associated with the radio axes, as expected in the unified schemes. Note, however, that the polarization properties of the integrated light do not constitute a proof of the unified schemes, because it is not possible to distinguish anisotropic radiation fields from anisotropic distributions of scatterers.

4.3 The origin of the redshift dependence

One of the most interesting results to emerge from this study is the redshift dependence of the polarization. There are three possible explanations for this dependence.

(i) *Dilution by old stars in the haloes of the host galaxies.* If the spectral energy distributions of the high-redshift radio galaxies consist of a scattered component that dominates in the UV and a component contributed by an old stellar population that dominates in the red, then the dilution of the polarization will increase sharply between rest wavelengths 3000–5000 Å, because the spectral energy distributions of old stellar populations show a sharp increase (a factor of 3–5 in F_λ) in this wavelength range. For observations in the V band, the 3000–5000 Å feature will be roughly centred in the middle of the band at a redshift of $z=0.4$, but by a redshift of 0.6 the feature will be centred at the red edge of the band. Thus, the observation of the large apparent increase in the polarization between $0.3<z<0.6$ can be explained as an effect of the rapidly diminishing dilution as the 3000–5000 Å feature moves towards the edge of the V band: for the low-redshift radio galaxies we are observing mainly the old stars, whereas for the high-redshift radio galaxies we are observing mainly the scattered light. The effect of the dilution by old stars will be enhanced by the wavelength dependence of the scattered light, which will rise steeply to the blue in the case of dust scattering (assuming scattering properties similar to those of dust grains in our own Galaxy). The low level of polarization in the red data for 3C441 is consistent with such dilution.

(ii) *Increasing beam power as a function of redshift.* From the strong correlation between radio power and redshift for 3C galaxies, and the separate correlation between radio power and emission-line luminosity (e.g. Rawlings & Saunders 1991), it is plausible that the strength of the illuminating radiation field increases with redshift. The amount of scattered light is directly proportional to the strength of the illuminating radiation field, so we expect some increase in the relative amount of scattered light (in the presence of other, diluting components) due to this effect as the redshift increases. This might explain some of the redshift dependence in Fig. 1, although we note that it cannot be the full explanation, because the low-redshift radio galaxy 3C405 (Cygnus A), which has a radio power comparable with the high-redshift objects, has only a moderate optical polarization (<2 per cent; Tadhunter *et al.* 1990).

(iii) *More effective scattering ISM at high redshifts.* The polarization also depends on the effectiveness of the scattering ISM. Fig. 1 might therefore be interpreted as an increase in the effectiveness of the scattering ISM as the redshift increases. This is an exciting possibility, because it implies a change in the properties of the ISM (e.g. the amount of dust) as a function of redshift, which would be some of the first direct evidence for evolution of the ISM in these galaxies.

Several independent strands of evidence already point to the importance of the dilution effect. By continuity with low-redshift radio sources, we expect the high-redshift radio sources to have early-type host galaxies with substantial haloes of old stars. Direct observational support for the dominance of an old stellar population in the optical/near-IR is provided by the general spectral energy distributions of the high-redshift objects (Chambers & Charlot 1990; Rigler *et al.* 1992), the small scatter on the infrared Hubble diagram for radio galaxies (Lilly 1989), the dilution of the polarization in the extended emission of 3C368 (Scarrott *et al.* 1990), and possibly also by the relatively low level of polarization measured in the no-filter observation of 3C441 (see above). We also have direct evidence from the continuum spectra of many low-redshift radio galaxies that they are dominated by old stellar populations at optical/near-IR wavelengths. Thus, dilution by old stars is likely to be important at optical/near-IR wavelengths in radio galaxies at all redshifts.

To determine whether dilution is the *dominant* effect, accurate measurements of the wavelength dependence of the polarization in individual high-redshift radio galaxies are required. Unfortunately, the existing data do not give a clear-cut answer: in 3C265 there appears to be little dilution with wavelength (Januzzi & Elston 1991), and although there is evidence for substantial dilution in 3C368 (di Serego Alighieri *et al.* 1989; Scarrott *et al.* 1990), there is the problem that much of this dilution might be caused by a foreground dwarf star in our own Galaxy (Hammer, Le Fèvre &

Proust 1991) and/or emission lines. We again caution that both 3C265 and 368 are extreme, and the scattered light may dominate over the diluting stars to a greater degree than in more typical high-redshift 3C radio galaxies.

5 CONCLUSIONS

The data show that large (rest frame) UV polarization is a relatively common feature of high-redshift ($z > 0.5$) radio galaxies. At the very least this suggests that caution is required in fitting the optical/UV colours and spectral energy distributions with pure starlight models.

We have also found that the occurrence of large (>5 per cent) optical polarization appears to increase dramatically between redshifts $z \sim 0.3$–0.6 (for galaxies observed in the V band). It is interesting that both the alignment effect (McCarthy *et al.* 1987) and the bluing effect in the optical/IR colours (Lilly & Longair 1984) begin to become prominent at similar redshifts. The most likely explanation for this redshift dependence is dilution by the starlight from old stars in the haloes of the host galaxies, combined with the overall wavelength dependence of the scattered light. Thus our observations are consistent with the suggestion (see in particular Rigler *et al.* 1992) that radio galaxies consist of an 'active' component which dominates in the UV and is aligned with the radio axis, and a 'passive' component which dominates in the optical/IR and is identified with the old stars in the haloes of the galaxies. The question of whether the active component is purely scattered light, or a mixture of scattered light and starlight, remains open.

ACKNOWLEDGMENTS

We thank the staff at the La Palma Observatory for the facilities and support during our observing run. SERC is acknowledged for continuing financial support of the Durham polarimetry group.

REFERENCES

Antonucci, R. R. J., 1984. *Astrophys. J.*, **278**, 499.
Barthel, P. D., 1989. *Astrophys. J.*, **336**, 606.
Chambers, K. C. & Charlot, S., 1990. *Astrophys. J. Lett.*, **348**, L9.
Chambers, K. C., Miley, G. K. & Joyce, R. R., 1988. *Astrophys. J. Lett.*, **329**, L75.
de Young, D. S., 1989. *Astrophys. J. Lett.*, **342**, L59.
di Serego Alighieri, S., Fosbury, R. A. E., Quinn, P. J. & Tadhunter, C. N., 1989. *Nature*, **341**, 307.
di Serego Alighieri, S., Binette, L., Courvoisier, T. J.-L., Fosbury, R. A. E. & Tadhunter, C. N., 1988. *Nature*, **334**, 591.
Draper, P. W., 1988. *PhD thesis*, University of Durham.
Eisenhardt, P. & Chokshi, A., 1990. *Astrophys. J. Lett.*, **351**, L9.
Fabian, A. C., 1989. *Mon. Not. R. astr. Soc.*, **238**, 41P.
Hammer, F., Le Fèvre, O. & Proust, D., 1991. *Astrophys. J.*, **374**, 91.
Januzzi, B. T. & Elston, R., 1991. *Astrophys. J. Lett.*, **366**, L69.
Lawrence, A. *et al.*, 1992. *Mon. Not. R. astr. Soc.*, submitted.
Lilly, S. J., 1989. *Astrophys. J.*, **340**, 77.
Lilly, S. J. & Longair, M. S., 1984. *Mon. Not. R. astr. Soc.*, **211**, 833.
Mannion, M. D. & Scarrott, S. M., 1984. *Mon. Not. R. astr. Soc.*, **208**, 905.
McCarthy, P. J., 1987. *PhD thesis*, University of California.
McCarthy, P. J. & Chambers, K. C., 1990. *Astrophys. J. Lett.*, **354**, L9.
McCarthy, P. J., van Breugel, W., Spinrad, H. & Djorgovski, S., 1987. *Astrophys. J. Lett.*, **321**, L29.
Orr, M. J. L. & Browne, I. W. A., 1984. *Mon. Not. R. astr. Soc.*, **200**, 1067.
Rawlings, S. & Saunders, R., 1991. *Nature*, **349**, 138.
Rees, M. J., 1989. *Mon. Not. R. astr. Soc.*, **239**, 1P.
Rigler, M. A., Lilly, S. J., Stockton, A., Hammer, F. & Le Fèvre, O., 1992. *Astrophys. J.*, in press.
Scarrott, S. M., Rolph, C. D. & Tadhunter, C. N., 1990. *Mon. Not. R. astr. Soc.*, **243**, 5P.
Scarrott, S. M., Warren-Smith, R. F., Pallister, W. S., Axon, D. J. & Bingham, R. G., 1983. *Mon. Not. R. astr. Soc.*, **204**, 1163.
Spinrad, H., Liebert, J., Smith, H. E. & Hunstead, R., 1976. *Astrophys. J. Lett.*, **206**, L79.
Spinrad, H., Djorgovski, S., Marr, J. & Aguilar, L., 1985. *Publs astr. Soc. Pacif.*, **97**, 932.
Tadhunter, C. N., 1990. In: *New Windows to the Universe, Vol. II*, p. 79, eds Sanchez, F. & Vazquez, M., Cambridge University Press, Cambridge.
Tadhunter, C. N., Scarrott, S. M. & Rolph, C. D., 1990. *Mon. Not. R. astr. Soc.*, **246**, 163.
Tadhunter, C. N., Fosbury, R. A. E., di Serego Alighieri, S., Bland, J., Danziger, I. J., Goss, W. M., McAdam, W. B. & Snijders, M. A. J., 1988a. *Mon. Not. R. astr. Soc.*, **219**, 555.
Tadhunter, C. N., Fosbury, R. A. E. & di Serego Alighieri, S., 1988b. In: *BL Lac Objects: Proceedings of the Como Conference 1988*, p. 79, eds Maraschi, L., Maccacaro, T. & Ulrich, M.-H., Springer-Verlag.
Warren-Smith, R. F., Scarrott, S. M., King, D. J., Taylor, K. N. R., Murdin, P. & Bingham, R. G., 1980. *Mon. Not. R. astr. Soc.*, **192**, 339.
Wright, J. S. & MacKay, C. D., 1981. *Proc. Soc. photo-opt. Instr. Eng.*, **290**, 160.